Supporting Information

Monajemi et al. 10.1073/pnas.1219540110

SI Text

1. Stat 330/CME 362 Collaboration. The researchers in Stat 330/CME 362 Fall 2011 who ran experiments for this collaboration include Sivaram Ambikasaran, Sergio Bacallado, Dinesh Bharadia, Yuxin Chen, Young Choi, Mainak Chowdhury, Soham Chowdhury, Anil Damle, Will Fithian, Georges Goetz, Logan Grosenick, Sam Gross, Gage Hills, Michael Hornstein, Milinda Lakkam, Jason Lee, Jian Li, Linxi Liu, Carlos Sing-Long, Mike Marx, Akshay Mittal, Hatef Monajemi, Albert No, Reza Omrani, Leonid Pekelis, Junjie Qin, Kevin S. Raines, Ernest Ryu, Andrew Saxe, Dai Shi, Keith Siilats, David Strauss, Gary Tang, Chaojun Wang, Zoey Zhou, and Zhen Zhu.

Also, M.G. was Teaching Assistant for Stanford course Stat 330/CME 362 in Fall of 2011 and helped organize the data and plan the experiments.

All these participants should be considered coauthors of this paper.

2. Named Authors. H.M., S.J., and M.G. also participated by amalgamating the data, preparing the analysis in this paper, framing the discussion of the final manuscript, or writing the manuscript.

D.L.D. designed the experiment, wrote some of the software, performed analysis, and coauthored the paper.

3. Additional Participant. Zulfikar Ahmed translated our code into python and replicated our experiments on PiCloud/Amazon Web Services. He should also be considered a coauthor of this collaboration at a level equal to the members of the Stat 330/CME 362 collaboration.

SI Appendix: Matrix Specifications

SS. The SS frame in the complex case is simply the n by $2n$ matrix (Eq. **S1**)

$$A = [I_n F_n], \qquad \textbf{[S1]}$$

where I_n is the n by n identity matrix, and F_n is the n by n unitary discrete Fourier transform matrix, with entries $F_{i,j} = \exp\{2\pi\sqrt{-1}ij/n\}/\sqrt{n}$. In the real case, $A_{n,2n} = [IR_n]$, where R_n is a real orthogonal n by n matrix, and the columns are each a normalized version of the real part or imaginary part of some corresponding column of F_n. The frame can be defined for any n. As noted in the text, we also considered these variants of real sinusoids: Hartley transform, Discrete Cosine Transforms (DCT) I, II, III, IV, with little change in results.

SH. The SH frame in all cases is simply the n by $2n$ matrix (Eq. **S2**)

$$A = [I_n H_n], \qquad \textbf{[S2]}$$

where I_n is the n by n identity matrix, and H_n is the n by n real orthogonal discrete Hadamard transform matrix. In principle, a wide range of n is possible for the Hadamard transform; in practice, we used only dyadic n, $n = 2^j$, and Hadamard matrices defined recursively by

$$H = 2^{-1/2}\cdot\begin{bmatrix} H_{n/2} & H_{n/2} \\ H_{n/2} & -H_{n/2} \end{bmatrix}.$$

SN. The SN frame in the complex case is the n by $2n$ matrix (Eq. **S3**)

$$A = [I_n W_n], \qquad \textbf{[S3]}$$

where I_n is the n by n identity matrix, and W_n is the n by n unitary matrix representing the discrete Noiselet transform (1). In the real case, W_n is replaced by an n by n real matrix R_n, and the columns are the nonredundant and normalized versions of the real and imaginary parts of columns of the complex matrix W_n.

PETF. The Paley frame was defined by Bandeira et al. (2) as follows. Let p be an odd prime and $N = p + 1$. From the usual orthonormal discrete Fourier transform matrix F_N, number the rows starting at zero and select only the rows corresponding to quadratic residues mod p. This will select $(p-1)/2$ rows deterministically. Append to this matrix a row of constants.

GF. The GFs that we use are defined in ref. 14 as follows. Let $n \geq 5$ be a prime integer, and let $a_t = \exp\{2\pi\sqrt{-1}t^3/n\}$ be the *Alltop* sequence, a quadratic-phase chirp. Let $A(\ell)$ denote the diagonal matrix with $A(\ell)_{ii} = a_{i-\ell}$. Let $N = n{\cdot}L$, and let F_n denote the usual orthonormal discrete Fourier transform matrix. Then, A is an $n \times N$ matrix defined by concatenating together the L block matrices $A(\ell)F_n$ (Eq. **S4**):

$$A = [A(0)F_n|A(1)F_n|A(2)F_n|\ldots|A(L-1)F_n]. \qquad \textbf{[S4]}$$

This frame is only considered for n prime and $0 < L < n$; it is then equiangular.

LC. The LC matrix that we use was defined in ref. 3. Let n be prime, and let $c_t^\ell = \exp\{2\pi\sqrt{-1}\ell t^2/n\}$ be the linear *Chirp* sequence with chirp rate ℓ. Let $C(\ell)$ denote the diagonal matrix with $C(\ell)_{tt} = c_t^\ell$. Let $N = n{\cdot}L$, and let F_n denote the usual orthonormal discrete Fourier transform matrix. Then, A is an $n \times N$ matrix defined by concatenating together the L block matrices $C(\ell)F_n$ (Eq. **S5**):

$$A = [C(0)F_n|C(1)F_n|C(2)F_n|\ldots|C(L-1)F_n]. \qquad \textbf{[S5]}$$

This frame is only considered for n prime and $1 < L < n$; it is then tight and equiangular.

DG. The DG frames that we use are defined in refs. 4 and 5 and called $DG(m,0)$ or Kerdock frames. Let m be an odd integer, let $n = 2^m$ be dyadic, and let $d_t^\ell = (\sqrt{-1})^{i(t)\,P_\ell\, i(t)}$ be the binary chirp based on the m by m binary symmetric matrix P_ℓ in the $DG(m,0)$ set, where $i(t)$ is the binary m-tuple bit vector encoding the value of $t \in \{0,\ldots,n-1\}$. Let $D(\ell)$ denote the diagonal matrix with $D(\ell)_{tt} = d_t^\ell$. Let $N = n{\cdot}L$, and let H_n denote the usual orthonormal discrete Hadamard transform matrix. Then, the complex-valued DG frame A is an $n \times N$ matrix defined by concatenating together the L block matrices $D(\ell)H_n$ (Eq. **S6**):

$$A = [D(0)H_n|D(1)H_n|D(2)H_n|\ldots|D(L-1)H_n]. \qquad \textbf{[S6]}$$

The real-valued DG frames are also defined in ref. 4. These are $2n$ by $2N$ matrices that are obtained by applying the Gray map to the corresponding complex-valued DG frames. Both real and complex DG frames are only considered for odd integer m, and $1 < L < n$. They are equiangular tight frames.

AC. Let $n = p^2$, where p is prime, and consider the affine plane $\mathbf{Z}_p^2$, with affine lines $\mathcal{L}_{a,b} = \{(i,j): j = a + bi \bmod p\}$ for $a, b \in \mathbf{Z}_p$, with line indicators $\chi_{a,b}(i,j)$. Let $a_\ell(i,j) = \exp\left\{\frac{2\pi\sqrt{-1}}{p}lij\right\}$ denote

a spatially chirping sinusoid. Let $\mathcal{L}_n$ denote the n by $n-1$ matrix, and the columns are all of the distinct $vec(\chi_{a,b})$ excluding $a=b=0$; let $\mathcal{A}(\ell)$ denote the n by n diagonal matrix with $vec(a_\ell)$ along the diagonal. Construct A by (Eq. **S7**)

$$A = [\mathcal{A}(0)\mathcal{L}_n|\mathcal{A}(1)\mathcal{L}_n|\mathcal{A}(2)\mathcal{L}_n|\ldots|\mathcal{A}(L-1)\mathcal{L}_n]. \qquad \textbf{[S7]}$$

This frame is neither tight nor equiangular. It has sparse columns and rows, with only $p=\sqrt{n}$ nonzeros in each and coherence $n^{-1/4}$, asymptotically much larger than the optimal value $n^{-1/2}$. We made this construction independently, but perhaps, the work in ref. 6 constructs this frame as well; we are not able to decipher the discussion in ref. 6.

1. Coifman R, Meyer Y, Geschwind F (2001) Noiselets. *Appl Comput Harmon Anal* 10(1): 27–44.
2. Bandeira A, Fickus M, Mixon D, Wong P (2012) The road to deterministic matrices with the restricted isometry propertyarXiv:12021234.
3. Applebaum L, Howard S, Searle S, Calderbank R (2009) Chirp sensing codes: Deterministic compressed sensing measurements for fast recovery. *Appl Comput Harmon Anal* 26(2): 283–290.
4. Jafarpour S (2011) Deterministic compressed sensing. PhD thesis (Princeton University, Princeton.
5. Calderbank AR, Howard S, Jafarpour S (2010) Construction of a large class of deterministic matrices that satisfy a statistical restricted isometry property. *IEEE J Sel Top Signal Process* 4(2):358–374.
6. Gurevich S, Hadani R, Sochen N (2008) The finite harmonic oscillator and its associated sequences. *Proc Natl Acad Sci USA* 105(29):9869–9873.

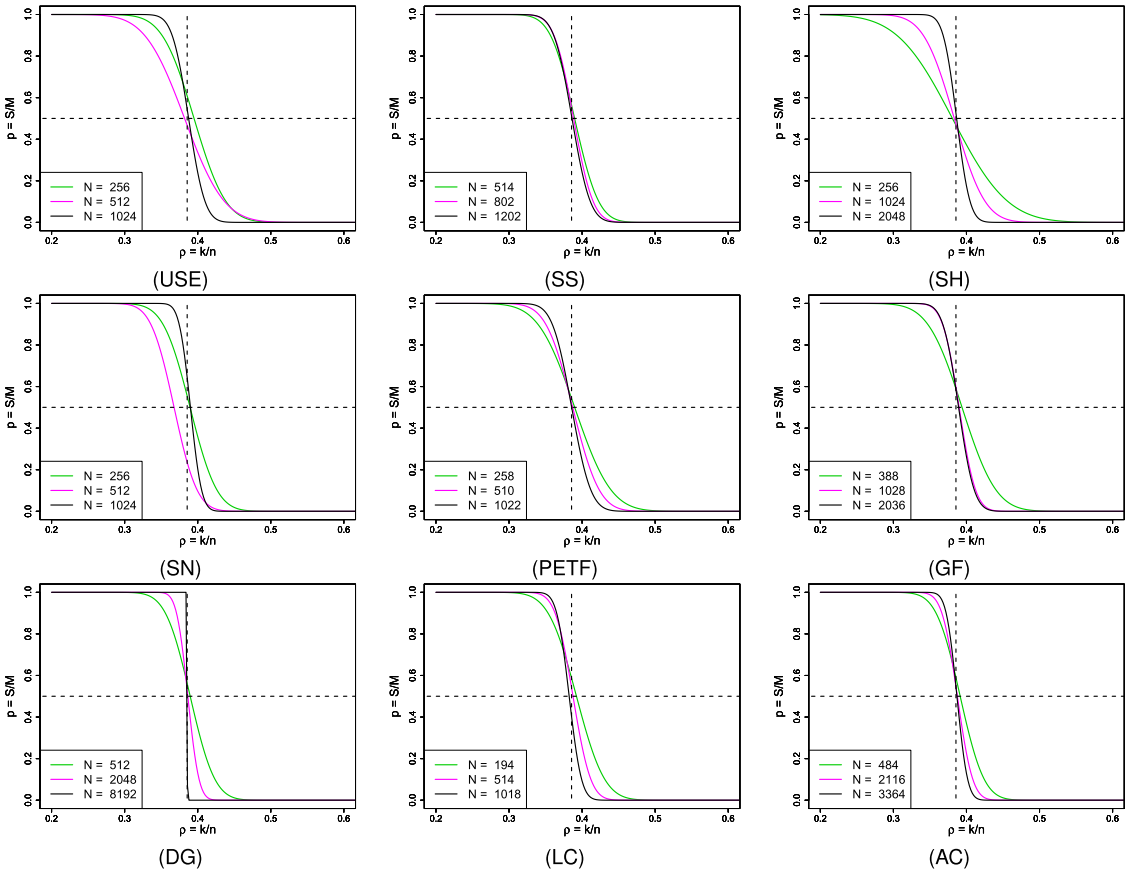

Fig. S1. Fitted success probabilities $\hat{\pi}(\rho\,|\,A_{n,N},\mathbf{R})$ for various matrices and problem sizes, all at undersampling ratio $\delta = 1/2$. In each panel, color encodes problem size. Green, smallest; blue, midmost; black, largest. Problem sizes: Gaussian (256, 512, 1,024); SS (514, 802, 1,202); SH (256, 1,024, 2,048); SN (256, 512, 1,024); PETF (258, 510, 1,022); GF (388, 1,028, 2,036); DG (512, 2,048, 8,192); LC (194, 514, 1,018); AC (484, 2,116, 3,364). The vertical dashed line locates the asymptotic phase transition for Gaussian ensembles. The horizontal dashed line locates the 50% success probability. In all cases, the tendency is for the curves associated with larger problem sizes to cross the 50% probability line near the theoretical phase transition for Gaussian matrices and the steepness of the transition to increase with *N*.

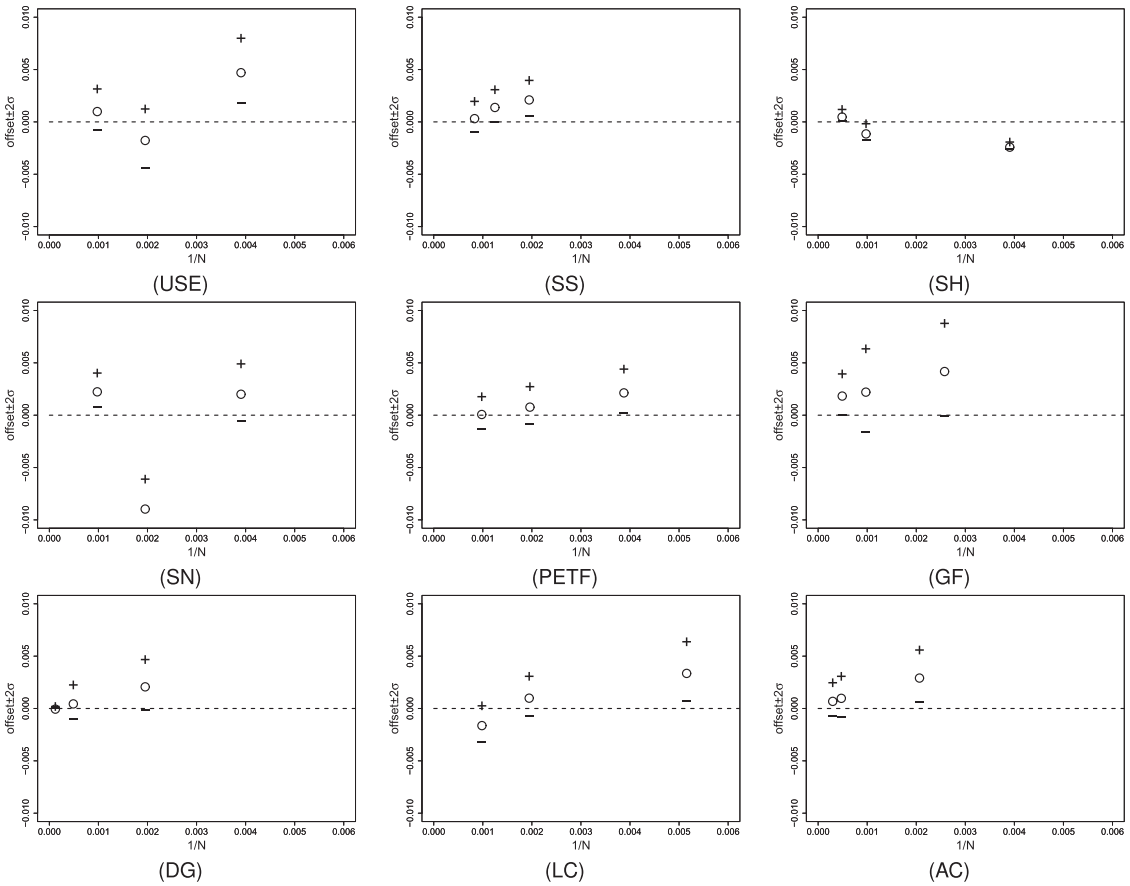

Fig. S2. Offset from asymptotic Gaussian phase transition, offset $= \hat{\rho}(n, N, M, \mathbf{R}) - \rho^*\left(\frac{1}{2}|\mathbf{R}\right)$, as a function of problem size N for coefficient set $\mathbf{X} = \mathbf{R}$ and $\delta = n/N = 1/2$: The x axis shows $1/N$, and the y axis shows offset $\pm 2S\,E(\text{offset})$. In each case, as N increases, we see that the interval gets closer to the asymptotic result indicated by the dashed line. Note that the label USE indicates behavior with initially Gaussian random matrices, which are then normalized so that all column norms are one; by mathematical theorems, results must agree in the $N \to \infty$ limit with the dashed line, and in finite problem sizes, there are empirical differences. The sizes of those empirical differences are consistent with empirical differences seen in all other cases.

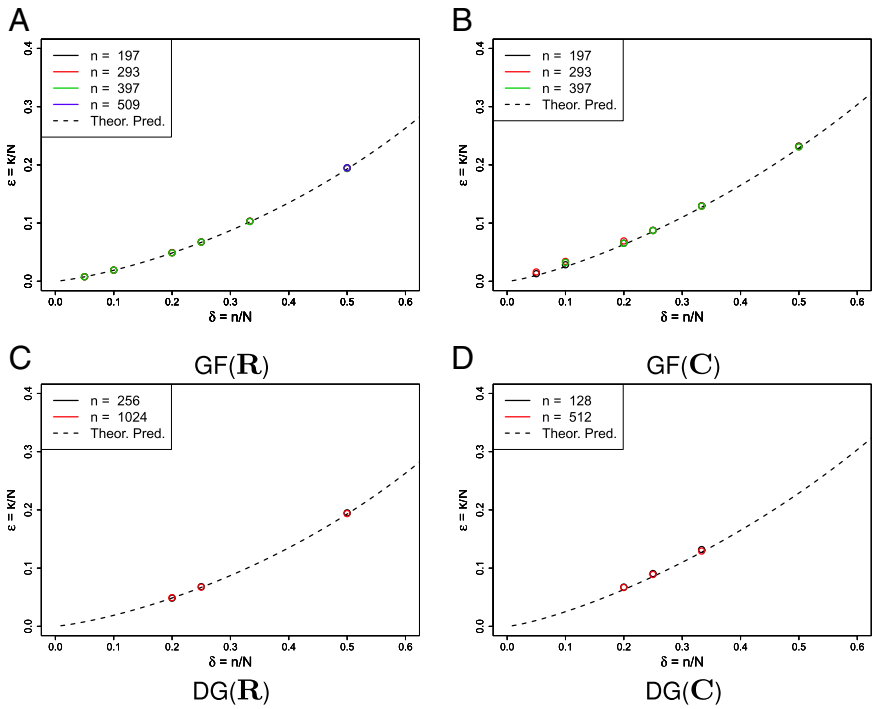

Fig. S3. Empirical phase transition curve for DG and GF: (*A*) GF (**R**), (*B*) GF (**C**), (*C*) DG (**R**), and (*D*) DG (**C**). In each panel, for certain δ, the location of 50% probability of success is denoted by circles. Asymptotic Gaussian phase transition $\rho^*(\delta|\mathbf{X})$ is indicated by the dashed curve in each panel for $X \in \{\mathbf{R}, \mathbf{C}\}$.